Updated Seismic Hazard Assessment Evaluation for the City of Aqaba, Jordan

Qadan, Hani [1*], Al Tarazi, Eid [2], Jaradat, Rasheed [3], Abu-Hamatteh, Ziad[1], Amjad, Yasin[1]

[1] *Civil Engineering Department, Faculty of Engineering Technology, Al-Balqa Applied University, Amman-Jordan*

[2] *Department of Earth and Environmental Sciences, Prince El-Hasan Bin Talal Faculty of Natural Resources and Environment, The Hashemite University, Zarka-Jordan*

[3] *Earth and Environmental Sciences Department, Faculty of Science, Yarmouk University, Irbid-Jordan*

Abstract

The Gulf of Aqaba area in Jordan is characterized by moderate to high seismic activity over the past 100 years in comparison to other parts of the Jordan-Dead Sea Transform. Nevertheless, some major earthquakes occurred in the area that affected the major cities of the Gulf such as Aqaba city. For the purposes of this study, nineteen active seismic sources were considered to assess the seismic hazard in Aqaba city. The Peak Ground Acceleration (PGA) and Response Spectra curves (RS) for different return periods (475, 975, and 2475 years) and nine selected sites representing different soil profiles in the city are determined. It is noted that 95% of the seismic hazard of the studied area is due to the sources lying within the influencing circle (i.e., ≤ 300 km). The calculated PGA value for a return period of 475 years was 0.3g. Meanwhile, it is considered in the Jordan Building Code as 0.2g. Furthermore, the PGA for return period of 975 years and 2475 years is 0.45g and 0.52g respectively. The results for soil profiles of hard rock and stiff soil for periods 0, 0.2, and 1 second were 0.3g, 0.7g, 0.2g, 0.35g, 0.79g, and 0.2g for a return period of 475 years respectively. It is calculated that the maximum spectral acceleration is 0.87g at Aqaba's southern coast for stiff soil profile, while its minimum value is 0.7g at the northern part of Aqaba for a return period of 475 years.

1. Introduction and Geologic setting

A seismic hazard refers to the likelihood of an earthquake, happening in a specific location, within a specific timeframe, with the intensity of the ground motion exceeding a specific threshold. This aids in estimating future risks, such that the decisions regarding building codes for typical structures, the design of infrastructure projects, land use planning, and insurance rates can be considered.

The strike-slip motion between the African plate and the Arabian plate is accommodated by the 'Jordan-Dead Sea Transform (JDST). The JDST extends into the Gulf of Aqaba, where the main rupture associated with the strike-slip mechanism is situated. These strike-slip type movements along the JDST occur when a fracture in the crustal rocks of the Earth, causing these rock masses to slide past one another parallel to the strike. It is due to these movements that the stress accumulates over time and gets a release in the form of earthquakes. (Al-Adamat and Diabat 2022). Results revealed that the existence of a strike-slip regime in all stress tensors. Three swarms within the Gulf of Aqaba occurred in 1983, 1990, and 1993 (Klinger *et al.,* 1999). The tectonic evaluation carried out through lineament and fracture analyses indicates that the regional development is tectonically related to the opening of the Red Sea, the development of the Dead Sea transform fault, and other distinct regional tectonic features. However, with a moment magnitude of Mw=7.1, the significant earthquake that struck

on November 22, 1995, marked the start of a seismic swarm that occurred in the central region of the Gulf of Aqaba. This seismic activity continued until December 31, 1997. It was thousands of small to moderate earthquakes that took place during this swarm. The Jordan Seismological Observatory recorded and examined 2089 of these earthquakes (Al-Tarazi and Qadan 1997; Al-Tarazi, 2000). The Gulf of Suez's rifting direction corresponds to the major trend of the extension stress pattern, which may be connected to the paleo stress that existed along the Gulf of Suez and Aqaba throughout the Middle to Late Miocene period (Abdel Fattah, *et al.,* 1997; Malkawi *et al.,* 1995; Abdelazim, *et al.,* 2023; Abou Karaki, *et al.,* 2022, Al-Amoush et al., 2017).

Moreover, it is assumed that at 2.3 ka, a catastrophic geological event, caused by down faulting in the northwestern edges of the Gulf of Aqaba, devastated the 'Elat' fringing coral reef. The encircling reefs at the northwest end of the gulf keep deteriorating over time due to damage brought on by down-throwing earthquakes (Shaked, *et al.,* 2004). More than 500 small local earthquakes (ML 4.85) occurred in the Gulf of Aqaba region between January 21 and April 20, 1983. The majority of the activity, including the greatest shocks, was confined to the region caused by strike-slip faults between latitudes 29°07′ and 29°15′ and longitudes 34°33′ and 34°42′. According to this data, the Gulf of Aqaba which is part of the JDST is characterized by seismic activity that falls into the foreshock-aftershock and swarm categories (El-

Isa, *et al.,* 1984). This seismic activity, resulting from the collision of the Arabian and African plates with the Eurasian plate, has greatly disturbed the tectonic framework of the JDST (ten-Brink and Ben-Avraham, 1989; Alvarado-Corona *et al.,* 2014).

In light of the extent of vigorous seismic activity in past situations. This study aims to determine and analyze the seismic hazard in the Aqaba City located in South Jordan using previously collected data to elaborate on the seismic risks, which may arise in the future.
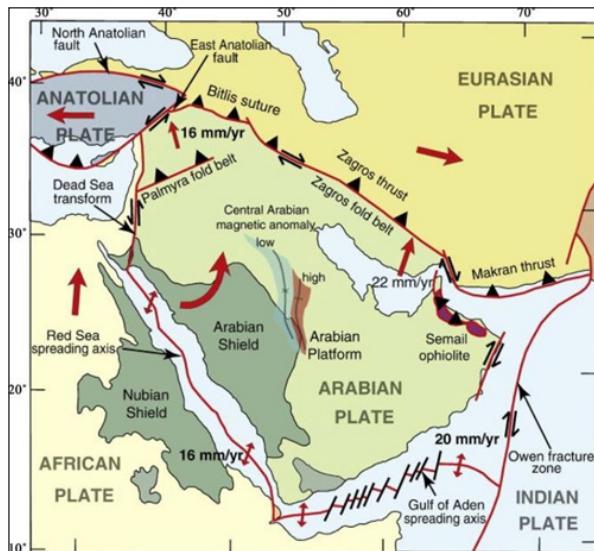
Figure 1. Regional tectonic of the Jordan Dead Sea Transform, indicating the movements and directions of the plate (Pascucci and Lubkowski, 2008).

2. Materials and Methods

2.1 Data Collection

Identification of the seismic sources in this study is dependent on the geology, local and regional tectonics, and historical and instrumental seismic data (Figure 1 and Figure 2). With delineation of these sources that depend on the uniformity of geotectonic features, the homogeneity of earthquake occurrences and consistency of its focal mechanism are shown in Figure 3. Seismic sources can be modeled as point, line, or area sources. In this investigation, the area source was adopted depending on Figures (1, 2, and 3), taking into consideration many previous studies of Al-Tarazi and Gruenthal (2003), Al-Tarazi (2005, 1994), El-Isa and Al Shanti (1989), Arieh and Rabinowitz, (1989), Garfunkel (1981). For the purpose of this study and depending on the above considerations to determine the seismic sources, 19 seismic area sources were identified and delineated as shown in Figure 4 and listed in Table 2. The influence of the seismic events located 300 km away from the study sites was considered negligible.

The seismic data was collected from several studies such as, USGS (2020), Al-Tarazi, (2003) Qadan, (1987), Jaradat *et al.,* (2008), Baaqeel *et al.,* (2016), Araya, and Armen, (1988) and Konstantinos *et al.,* (2019). The seismic events used in this study date back to 4000 years ago. Two types of data were collected, namely historical data from 31 BC until 1899

AD as shown in Figure 5 and data regarding instrumental earthquakes covering period from 1903 to 2019, specified in Figure 6.
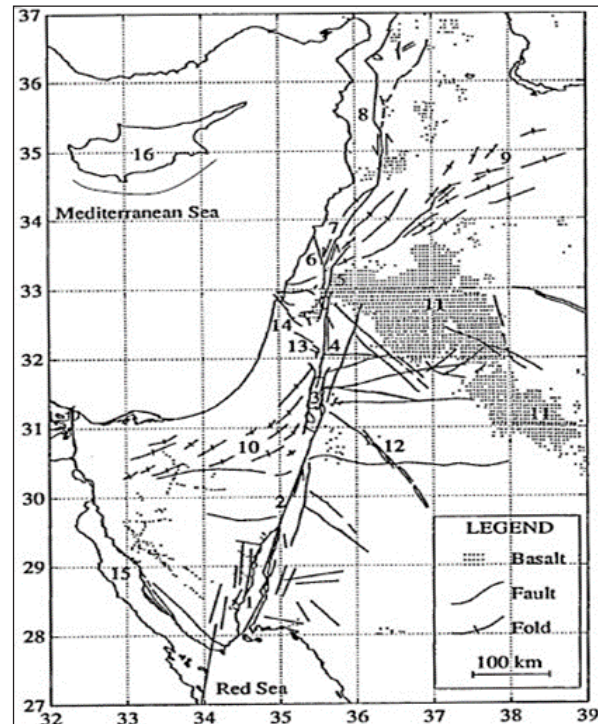
Figure 2. The Tectonic Map of Jordan and Vicinity. (1) Aqaba Gulf fault, (2) Wadi Araba fault, (3) Dead Sea Basin, (4) Jordan River Fault and Tiberias, (5) Rachaya Fault, (6) Ed Damur fault, (7) Yammouneh Fault, (8) Ghab Fault, (9) Palmyra Fold Belt, (10) Levantine Fold Belt, (11) Wadi Sirhan Graben, (12) Karak-Fayha Fault, (13) Farah Fault, (14) Al Karmel Fault, (15) Suez fault, (16) Cyprus (after Al-Tarazi, 1992).
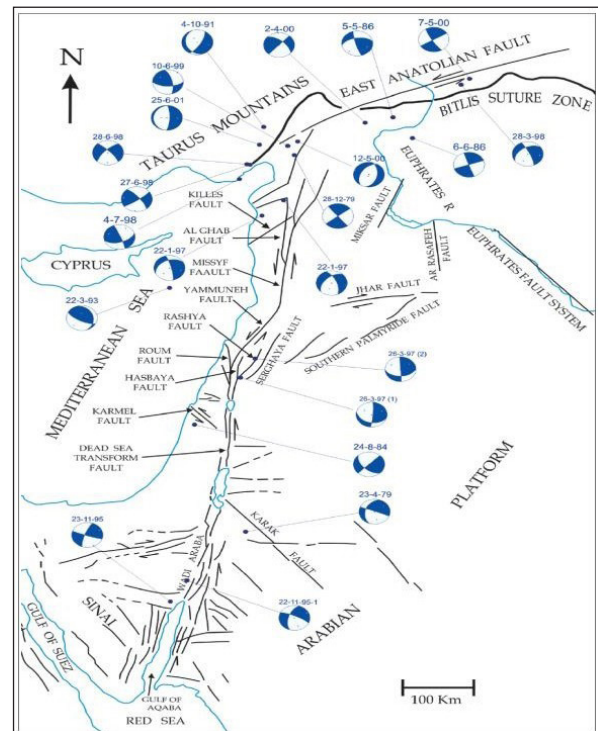
Figure 3. Summary of major fault zones of the northern Arabian plate (after Sbeinati *et al.,* 2005).
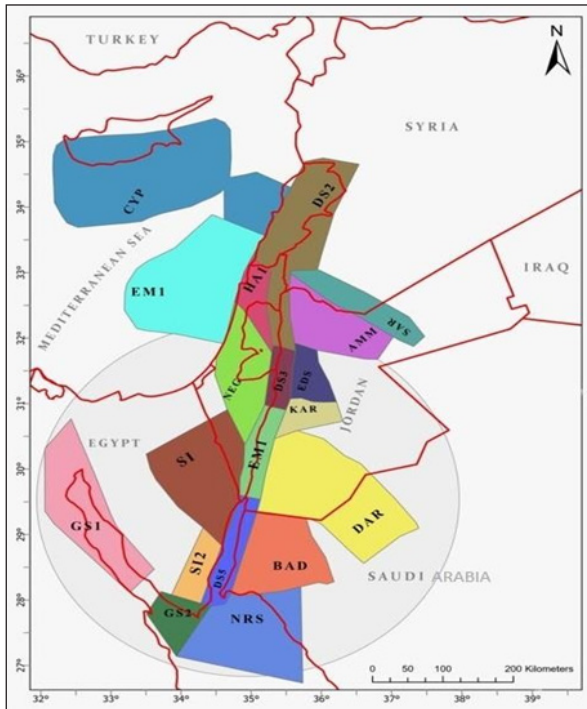
Figure 4. Area source model showing 19 seismic area sources delineated for the purpose of this study (Modified after Al-Tarazi and Gruenthal, 2003).
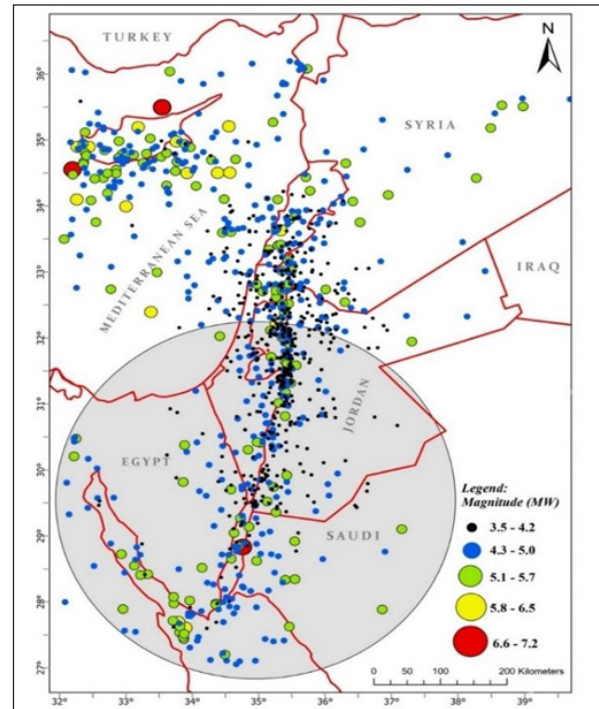

Figure 5. Epicenters of instrumental main earthquakes occurred in the JDST and around, during the period 1903 to 2019 and used in this study.

Table 1. Calculated Seismic Hazard Parameters for the 19 seismic sources.

No.	Source	a	b	β	λ4	M_{max} (M_w)	Max. Focal depth (Km)	Min. Focal depth (Km)
1	Amman (AMM)	2.7787	0.7085	1.6311	0.88044	5.5	40	10
2	Eastern Gulf of Aqaba (BAD)	1.1315	0.4239	0.9760	0.2728	5.5	21	10
3	Cyprus (CYP)	3.7388	0.861	1.9825	2.4819	7	67	20
4	Southeast of Jordan (DAR)	3.1739	0.8183	1.8842	0.0035	5.5	39	10
5	Northern Dead Sea (DS2)	3.9613	0.9569	2.2033	1.3605	7.6	33	10
6	Dead Sea Basin (DS3)	4.5687	1.119	2.576	1.2376	7.6	33	10
7	Gulf of Aqaba (DS5)	2.379	0.6398	1.4732	0.6604	7.0	33	10
8	East Dead Sea (EDS)	1.5625	0.4437	1.0216	0.6133	5.5	10	10
9	Wadi Araba (DS4)	3.6411	0.9853	2.2687	0.5010	7.0	25	10
10	Suez Gulf-1 (GS1)	1.6516	0.5673	1.3062	0.2412	6.5	33	20
11	Suez Gulf -2 (GS2)	2.8141	0.7327	1.6871	0.7644	6.5	39	20
12	Haifa Zone (HA1)	3.4686	0.9331	2.1485	0.5447	5.5	22	10
13	Karak Zone (KAR)	4.9904	1.2041	2.7725	1.4928	5.5	20	10
14	Naqab Zone (NEG)	6.0801	1.5315	3.5264	0.8997	5.5	23	10
15	Sarhan Zone (SAR)	2.2645	0.7404	1.7048	0.2009	6	28	10
16	Central Sinai Zone (SI)	2.4457	0.6604	1.5206	0.6369	5.5	24	10
17	Eastern Mediterranean (EM1)	3.8114	0.9694	2.2321	0.8586	7.7	31	10
18	South Saini (SI2)	0.9833	0.4771	1.0985	0.1188	5.5	14	10
19	Northern Red Sea (NRS)	5.4217	1.269	2.9862	1.7143	6	26	10
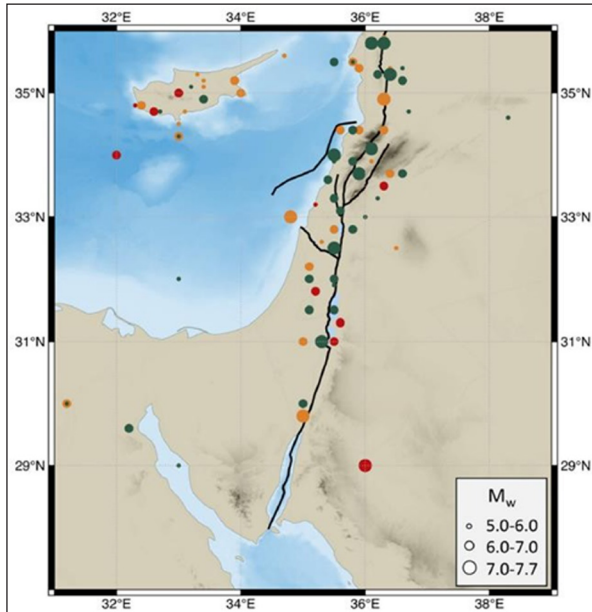
Figure 6. Map with all earthquakes with magnitudes Mw≥5 between 31 BC and 1900, inside our investigated zone (Gardner and Knopoff, 1974).

Gardner and Knopoff (1974). Clustering was used to remove the foreshocks and aftershocks from the data collected. An approximation of the windows sizes according to Gardner and Knopoff (1974) is shown in the following equations:

$$D_i = 10^{0.1238M+0.983} \tag{1}$$

For M≥6.5

$$Ti = 10^{0.038M+2.7389} \tag{2}$$

Else

$$Ti = 10^{0.5409M-0.547} \tag{3}$$

Where Di is a distance in Km and Ti is time in days.

Based on these equations, the size of the window for each magnitude interval is determined and listed in Table 2.

Table 2. Threshold values of distance (Di) and time (Ti) for the identification of foreshocks and aftershocks following the window method approach (Campbell and Bozorgnia, 2014).

Mw	Di (Km)	Ti (Days)
4.0-4.4	30	42
4.5-4.9	35	83
5.0-5.4	40	155
5.5-5.9	47	290
6.0-6.4	54	510
6.5-6.9	61	790
7.0-7.4	70	915
7.5-7.9	81	960
8.0-8.4	94	985

Based on this criterion, a software using Matlab™ was prepared to identify the main shocks of the earthquakes catalog used in this study. Additionally, alternative window parameter settings proposed by others of Matlab™ code (CORSSA Website; Al-Taani, 2011) were used (Campbell and Bozorgnia, 2014). The online supplement to this article provides codes written in Java as well as Matlab™.

2.2 Probabilistic Seismic Hazard Assessment Model

The calculations of the seismic hazard procedures considered by this study are summarized in the following:

2.2.1 Linear Gutenberg -Richter relationship:

The frequency of the occurrence of earthquakes was determined by the linear Gutenberg-Richter relationship:

$$\text{Log } N (m) = a - bm \tag{4}$$

Where log is the logarithm, having a base of 10, N (m) is the number of the shocks having magnitude equal to or greater than m. Over a given time interval, a and b are constants to be determined from the available data for the region using standard least squares method. Equation (4) can be rewritten as:

$$N(m) = e^{a-\beta m} \tag{5}$$

Where a= a ln 10 and $\beta = b$ ln 10 (where ln is natural logarithm). To take into consideration the incompleteness of data in the prepared earthquake catalog, for the assessment of constants *a* and *b* and consequently α and β for all seismic sources, Stepp's method was adopted. The calculation sample for the Gulf of Aqaba seismic source is shown in Figure 7.

The same procedure was used to determine the parameter β for the nineteen seismic active sources delineated in this study as listed in Table 2.
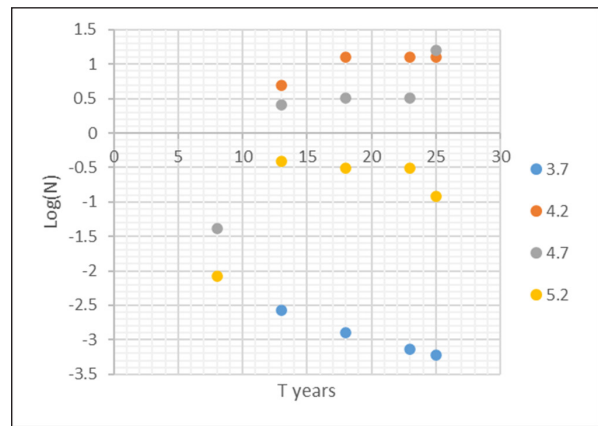
(a) Variation of a number of earthquakes in a period.
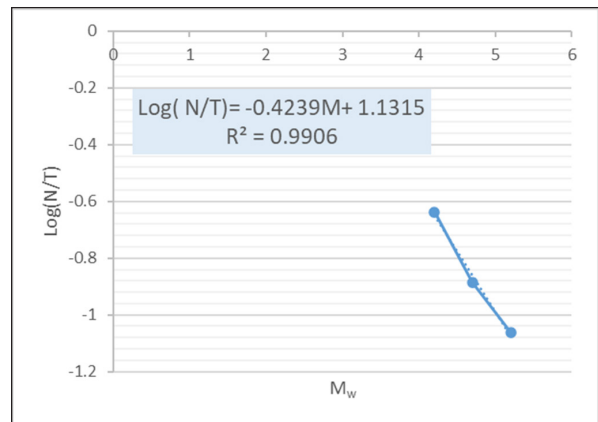
(b) Gutenberg - Richter relationship

Figure 7. Stepps' Method Applied for Eastern Gulf of Aqaba Seismic Source.

2.2.2 Annual Rate of Seismic Activity:

In this study, the minimum earthquake magnitude considered for engineering interests is M_w=4. Thus, the number of main shocks exceeding magnitude 4 is taken as in the following:

$$\lambda 4 = e^{a-4\beta} \tag{6}$$

2.2.3 Poisson's Distribution

Qadan (1987) showed that the occurrence of the main shocks of earthquake events is independent. In order to determine this, they used the X^2 statistics test for the intendance of earthquake events, so Poisson's distribution is adopted using:

$$P(n,t) = \frac{\lambda t e^{\lambda t}}{n!} \tag{7}$$

Where:

(n, t) = the probability of occurrence of n earthquakes in a time.

λ = the mean rate of earthquake occurrences per unit of time, which is generally taken as one year.

2.3 The maximum expected magnitude (Mmax):

The value of the maximum expected earthquake for each seismic source (Mmax) can be estimated using different methods. None of these methods is reliable, including the rupture length-magnitude and slip-magnitude relationships. So, in this research, (Mmax) was determined for each source depending on the utilized historical earthquake catalog. The maximum observed magnitude for each source was taken as the maximum expected magnitude. The minimum bound earthquake magnitude (Mmin) was selected in such a way that any earthquake below that magnitude is not of engineering interest or that the statistical data is not reliable and complete[23], which is equal to 4 for all seismic sources. Furthermore, the minimum and the maximum focal depth for each seismic source were determined and considered in the calculations of the hazard in this study as listed in Table 2. Depending on the above considerations, the seismic hazard parameters were calculated for each seismic source based on the data collected. The data was then checked, using the related equations mentioned above.

2.4 Attenuation Equation Models

Campbell and Bozorgnia (2014) investigated and developed a new ground motion prediction equation for the average horizontal components of PGA, PGV, and linear pseudo-absolute acceleration response spectra at 21 periods ranging from 0.01 s to 10 s corresponding to 5% damped. Furthermore, Darvasi and Agnon (2019) calibrated a new attenuation curve for the Dead Sea region using surface wave dispersion surveys in sites damaged by the 1927 Jericho earthquake.

To select a suitable attenuation equation for the seismic hazard analysis, the researchers referred to the collection of ground motion prediction equations by Douglas *et al.,* (2006). The most suitable attenuation equations in this region are already utilized in the studies of Abrahamson and Silva (2008; 2009), Boore, and Atkinson (2008), in terms of Peak Ground Acceleration (PGA). The choice of these two

equations is due to the following reasons:

- They took into consideration the engineering soil profile by considering the shear wave velocity Vs30 which is adopted in the international building codes.

- The equations are applicable for the Mw range of 5 to 8.5 strike-slip faults, including the maximum earthquakes considered in this study (Table 2).

- The actual peak ground acceleration Ya=N1Y, where Log N1 is a random variable normal distribution with a mean value of zero and standard deviation ranging from 0.5 to 1.05 (Araya, and Armen, 1988).

The final step in the seismic hazard analysis is to calculate the seismic hazard for the area under consideration using the area source model (Paz and Leigh 2004).

$$P(Y > y) = \sum_{i=1}^{n} \frac{v_i}{v} \iint_{M\,R} P(Y > y|m,r) f_{R|M}\,dr f_M(m)\,dm \tag{8}$$

$$T_y = \frac{1}{vP(Y>y)} \tag{9}$$

Where P [Y>y] is the probability that a random site peak ground acceleration (Y) at the site will exceed a certain acceleration (y) and T_y is the return period of a certain acceleration y. Given the location (r) and the closest length of rupture (*R*), the nearest distance from the rupture to the site is calculated. Integration over m, *r,* and y gives the total probability that Y will be exceeded due to a single event of random variables M, R, and Y.

3. Results and Discussion

The resulting hazard parameters are listed in Table 2 shown below. The maximum expected magnitude (Mw) values are also given along with the maximum and minimum focal depth (km).

3.1 Peak Ground Acceleration (PGA)

Most districts of Aqaba have soil profiles of hard rock (SA) or stiff soil (SD) as reported by ASEZA (2010) and shown in Fig. 8 and Table 3. This classification is based on Jordan National Building Code for Seismic Resisting Design (JBC). The shear wave velocity for soil profiles of SA and SD ranges between 760 to 1500 m/s and 180 to 360 m/s respectively. Another parameter is the thickness of the sediments covering the bedrock (Z1). Physically, Z1 represents the depth at which the shear wave velocity equals 1000 m/s. Z1 value is zero for the hard rock site profile and 600 m for the stiff soil site profile (Table 3). Site E is selected to represent the rest of the sites due to its important location as it represents the center of the city.

The analysis which is carried out based on the seismicity parameters of seismic sources is shown in Fig. 4 and Table 2. Two attenuation equations were used to evaluate the seismic hazard (Boore and Atkinson, 2008; Yucmen, 1977) for the nine sites representing different areas in Aqaba (Figure 5). Their coordinates and soil profile properties for each site are listed in Table 3. A software EZ FRISK was used for this purpose. The results of the analysis indicate that the average values of the PGA are closer to Abrahamson and Silva's (2009) attenuation equation.
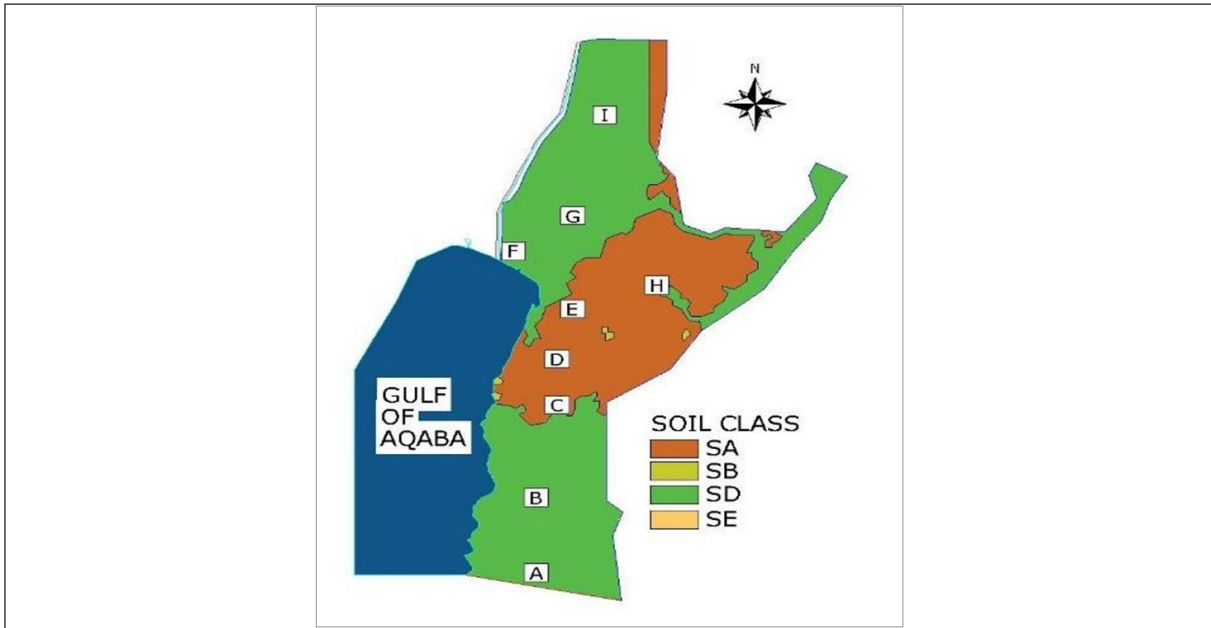
Figure 8. The soil profile classification and distribution in Aqaba city and around (SA: Hard rock, SB: Rock, SD: Stiff soil profile, and SE: Soft soil profile). (A-I) are the locations of the nine sites studied.

Table 3. Coordinates and soil profile properties of the nine studied sites in Aqaba and its vicinity.

Site	Latitude	Longitude	Soil Profile	Ca	Cv	Vs1	Z11	Vs2	Z12
A	29°21'57.58"N	34°58'27.77"E	SD	0.28	0.4	270	600	760	0
B	29°24'59.39"N	34°58'45.55"E	SD	0.28	0.4	270	600	760	0
C	29°28'50.47"N	34°59'23.72"E	SA	0.16	0.16	760	0	NA	NA
D	29°30'33.69"N	34°59'59.20"E	SA	0.16	0.16	760	0	NA	NA
E	29°32'10.23"N	35° 0'24.67"E	SD	0.28	0.4	270	600	760	0
F	29°32'34.83"N	34°58'58.44"E	SD	0.28	0.4	270	600	760	0
G	29°34'6.94"N	34°58'59.36"E	SD	0.28	0.4	270	600	760	0
H	29°33'3.83"N	35° 1'30.06"E	SA	0.16	0.16	760	0	NA	NA
I	29°36'29.56"N	35° 1'6.53"E	SD	0.28	0.4	270	600	760	0

Where: C_a is the acceleration coefficient according to the UBC-97 code. C_v is the velocity coefficient according to the UBC-97 code. V_{s1} and V_{s2} are the seismic shear wave velocities at different depths in m/s and represent soil profiles of SA and SD respectively. Z_{11} and Z_{12} are the depth at which the shear wave velocity is equal to 1000 m/s corresponding to V_{s1} and V_{s2} respectively.

A sample of the resulting hazard curves is shown in Figures 9 and Figure 10. It was observed that the PGA in Aqaba ranges from 0.3g to 0.4g corresponding to a return period of 475 years. Furthermore, Table 4 lists the results taken from the derived curves showing the return period corresponding to PGA for different soil profiles, where the PGA values for the SD profile are higher than that of the SA profile for site E. Furthermore, the present study covers a wider range of PGA in the comparison done by Qadan (1987). This is due to more refined input data.
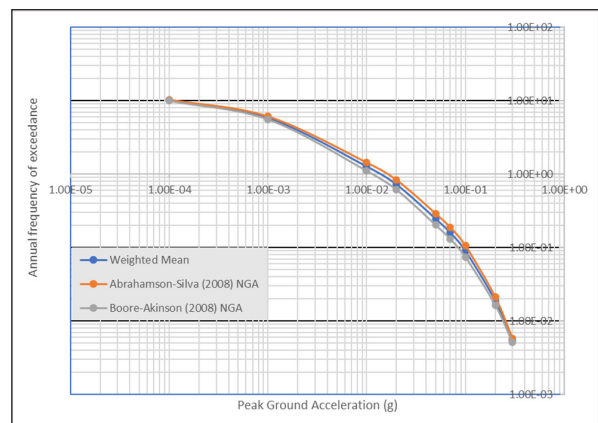
Figure 9. Total mean hazard of average horizontal component of Peak Ground Acceleration (weighted average) for site E in Aqaba, compared to Abrahamson and Silva (2009), and Boore and Atkinson (2008), attenuation equations results.

Table 4. Calculated PGA of site E at the center of Aqaba city.

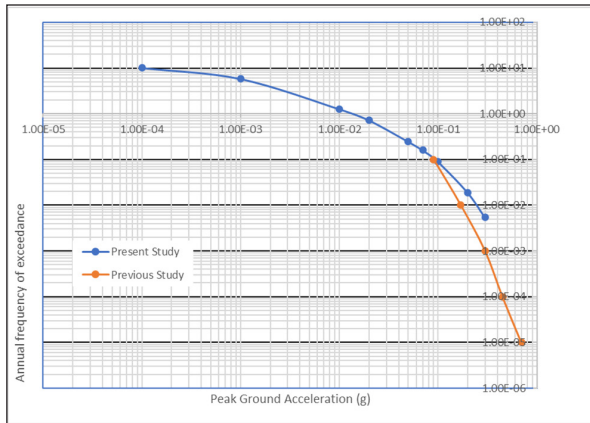| Probability of Exceedance (return period)	PGA (g), Vs=270 m/s, Z1=600m	PGA (g), Vs=760m/s, Z1=0
10% (475 years)	0.3	0.4
5% (975 years)	0.4	0.45
2% (2475 years)	0.5	0.52

Figure 10. Comparison of this study to Qadan study (1987).

3.2 Response Spectra Curves for Aqaba City

Originally, the derivation of response spectra curves is performed by calculating the response excitation of single degree of freedom system, which depends on the strong motion records of major earthquakes (JBC, 2005). Moreover, the international building codes derive the response spectra by assessment of PGA using the seismic hazard analysis (corresponding to return period of 475 years) in relation to the soil profile type. Usually, seismic response spectra curves are used in the international building codes for seismic design of engineering structures for return period of 475 years (10% of being exceeded in 50 years). Other curves of different return periods are used for more important facilities like dams and nuclear power plants. A further set of results of this study was calculated for response spectra curves for 5% damping, corresponding to different return periods of 475, 975, and 2475 years, for the nine selected sites. A sample of these resulted curves is shown in Figure 11.

The response spectra curves for Aqaba city based on JBC for seismic design are shown in Figure12. These curves are originally based on PGA= 0.2g (Zone 2B) which correspond

to a return period of 475 years as derived from Jordan zoning map, and soil profiles of SA and SD.

Table. 5 compares the Spectral Acceleration of this study (Figure 11) and the corresponding values for Aqaba based on JBC (Figure12) for spectral periods 0, 0.2, and 1 second. The values are very close except for the spectral acceleration corresponding to 1 second, which is 33% more than JBC (2005) value. This difference may be due to refined and updated input data used in the analysis of this study considering the site effects of the studied area. Figure 13 shows the comparison of response spectra of the present and the JBC (2005) code for Site E.
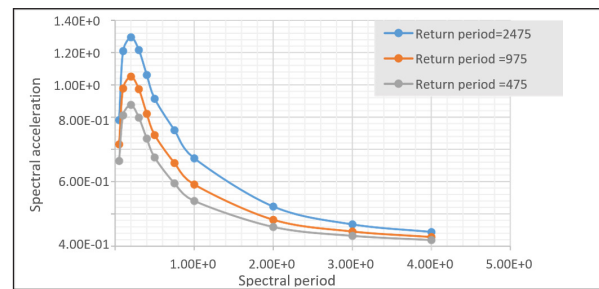

Figure 11. Calculated Response Spectra of average horizontal component acceleration for 5% damping for return periods of (475, 975, and 2475 years) for site E.
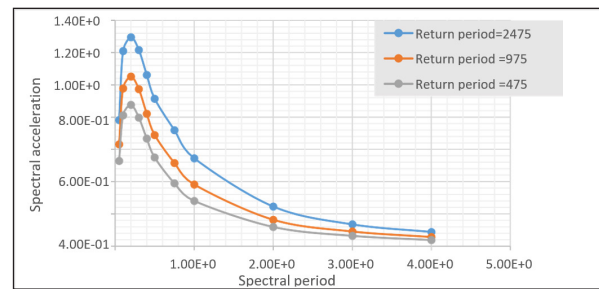

Figure 12. Response Spectra for different soil profiles at Aqaba city (zone 2B) as per JBC (2005).

Table 5. Spectral acceleration results of the values investigated sites within the study area compared to those listed in the national building code (JBC 2005).

| Site	Soil Profile	SA @ t=0 s	SA @t= 0.2s	SA@ t= 1s	PGA (475 years)
A	SD	0.35	0.87	0.21	0.35
B	SD	0.35	0.8	0.20	0.35
C	SA	0.35	0.75	0.20	0.35
D	SA	0.35	0.75	0.20	0.30
E	SD	0.40	0.86	0.30	0.35
F	SD	0.30	0.75	0.20	0.3
G	SD	0.35	0.70	0.14	0.35
H	SA	0.30	0.75	0.15	0.3
I	SD	0.35	0.70	0.15	0.35
JBC for Aqaba	SD	0.30	0.70	0.40	0.20
JBC for Aqaba	SA	0.16	0.40	0.17	0.20

As shown in Figure13, the higher mode of acceleration for the derived curve is less than the JBC response spectra. On the other hand, the fundamental acceleration in the derived response spectra is more than that of the JBC code. Spectral acceleration range for current study is (0.3-.86) g, while it is (0.4-0.7) g for JBC code. Moreover, high frequency

resulted from some earthquakes, produces high acceleration. For more study that is refined using logic tree structure will estimate more realistic output and consequently more refined response spectra curves.

In the design of multistory buildings, the design is mostly controlled by dynamic analysis. In this case, for higher
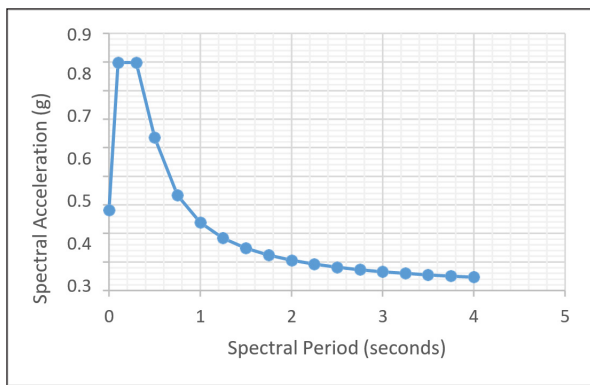
modes, the spectral acceleration is less than the fundamental mode acceleration.
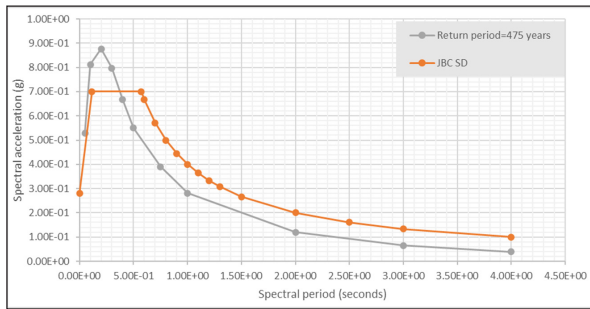
Figure 13. Comparison of response spectra of this study and the JBC (2005) code for Site E

Figure 14 shows a proposed response spectrum for a combination of the results of this study and the JBC curve.
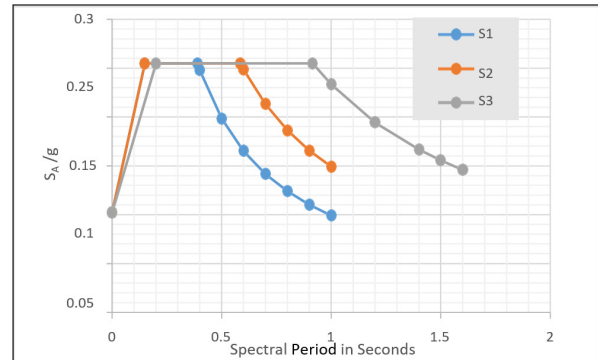

Figure 14. Proposed Response Spectra for Site E.

A set of response spectral curves are prepared for Aqaba city (north coast) using data collected from Nuweiba earthquake 1995 $M_W=7.1$ (Al-Tarazi, 2000) that affected Aqaba city for different soil profiles (results shown in Figure 10). The spectral acceleration values obtained from Figure 10 equaling 0.13 g are generally in agreement with the readings of the shoreline strong motion stations for the 1995 earthquake (0.16 g) (Al-Tarazi, 2000). The slight difference is due to the location accuracy of the strong motion station, which recorded the event. Furthermore, Fig. 15 and Table 6 also show the response spectra of three soil profiles S1 (Rock and stiff soil), S2 (Deep cohesion less or stiff clay soils), and S3 (Soft to medium clays and sands). The period of the peak spectral acceleration S1 is smaller than that of the same value for soil profiles S2 and S3. This phenomenon helps in the structural design of buildings to resist major earthquakes.

Table 6 lists the spectral acceleration values for different spectral periods (0.0, 0.2 and 1.0 second) from Figure 8, for site E. Moreover, these values are compared to the response spectra acceleration values, which are determined for Gulf of Aqaba earthquake (Figure 15).

It is noted that the spectral acceleration values at the critical points (i.e., t=0.0, 0.2, 1.0 second) are less than the current study values. This is due to the calculation of spectral acceleration in this study which is based on many seismic sources and wide range of earthquake data. Therefore, the results of this study are expected to be more realistic compared to the calculations of Nuweiba earthquake of 1995.

Figure 15. Response Spectra for Nuweiba earthquake 1995 for different soil profiles at the coastline.

Table 6. Comparison between the spectral acceleration of this study for site E with the effects of the Nuweiba earthquake 1995.

Site	Soil Profile	S_A at t=0 s	S_A at t= 0.2s	S_A at t= 1s
E (This Study)	SD	0.40	0.86	0.3
1995 ($M_W=7.1$)	S1	0.1	0.25	0.15
	S2	0.1	0.23	0.1
	S3	0.1	0.25	0.23

4. Conclusion

The results of this study could be summarized as follows:

1- The PGA value for 10% of being exceeded in 50 years (475 years return period) is (0.3-0.4) g. Meanwhile, the PGA for JBC for earthquake loads is 0.2g only (i.e., JBC is underestimating the seismic hazard.

2- The PGA value of 5% which is being exceeded in 50 years (975 years return period) is in the range from (0.45to 0.50) g, while for 2% which is being exceeded in 50 years (2475 years return period) is in the range from (0.56 to 0.6) g.

3- The results of response spectra for soil profile SA for site E for spectral periods 0, 0.2, and 1 second are 0.3g, 0.7g, and 0.2 g, respectively.

4- The results of response spectra for soil profile SD for site E for spectral periods 0, 0.2, and 1 second are 0.35g, 0.79g, and 0.2 g, respectively.

5- The response spectra for the rest of the studied sites of the spectral period zero range between (0.3 to 0.4) g, for a spectral period 0.2-second range (0.7 to 0.87) g, and spectral period 1-second range (0.15 to 0.21) g.

6- The JBC response spectra for soil profile SA for spectral periods 0, 0.2, and 1 second is 0.17g, 0.4g, and 0.16g respectively, while for soil profile SD for spectral periods 0, 0.2, and 1 second are 0.3g, 0.7g, and 0.4g respectively.

Conflict of Interest

The authors declare no conflict of interest.

References

Abdallah I. Husein (Malkawi); Azm S. Al-Homoud; Eid Al-Tarazi, and Osama K. Nusier (1995). Probabilistic Seismogenic Ground Motion Hazard Assessment of Karak City in Jordan, Environmental and Engineering Geoscience I (2): 207–218. https://doi.org/10.2113/gseegeosci.I.2.207.

Abdel Fattah, A. K., Hussein, H.M., Ibrahim, E.M. and Abu El Atta, A.S. (1997). Fault plane solutions of the 1993 and 1995 Gulf of Aqaba earthquakes and their tectonic implications. www.earth-prints.org. [online] Available at: https://www.earth-prints.org/handle/2122/1592.

Abrahamson and Silva, W. (2008). Summary of the Abrahamson and Silva NGA ground-motion relations. Earthquake Spectra, 24 (1): 67-97, doi: 10.1193/1.2924360.

Abrahamson and Silva, W. (2009). Errata for Summary of the Abrahamson and Silva NGA ground-motion relations by Abrahamson, N. A. and W. J. Silva. Published on PEER NGA website.

Al-Amoush, H.; Rajab, J. Abu; Al-Tarazi, E., 2017, Electrical Resistivity Tomography modeling of vertical lithological contact using different electrode configurations, Jordan Journal of Earth and Environmental Sciences (JJEES), 8, 1, 27-34.

Al-Tanni, A. A. (2011). Seismic Hazarder Assessment of the Middle East Region Unpublished M.Sc. Dissertation, Yarmouk University, Jordan, pp. 208.

Al-Tarazi, E. (1992). Investigation and Assessment of Seismic Hazard in Jordan and its Vicinity, Ph.D. Thesis. Institute of Geophysics, Ruhr University Bochum, Germany, 192 (unpublished).

Al-Tarazi, E. (1994). Seismic Hazard Assessment in Jordan and Its Vicinity, Natural Hazards, 10: 79-96.

Al-Tarazi, E. (2000). The Major Gulf of the Aqaba Earthquake, (1995) Maximum Intensity Distribution Natural Hazards 22: 17–27. doi:10.1023/a:1008109810031.

Al-Tarazi, E. (2003). Estimation of Horizontal Response Spectra and Peak Acceleration of Major Cities in Jordan. Fourth International Conference of Earthquake Engineering and Seismology. Tehran – Islamic Republic of Iran.

Al-Tarazi, E, and H., Qadan (1997). Seismic hazard potential expected for dams in Jordan, Dirasat (Natural and Engineering Sciences), 24, 313-325.

Al-Tarazi, E, 2005, Investigation of the effects of earthquake swarms in the seismic hazard in the Gulf of Aqaba, Northern Red Sea, Dirasat Pure Sci., 1, 55-68.

Al-Tarazi, E., Gruenthal, G. (2003). Seismic Hazard Estimation in Jordan and around, GFZ, 24 P, Un-Published report.

Alvarado-Corona R., Mota-Hernández C., Félix-Hernández, J. L. and Santos-Reyes J., (2014). What Can Be Learnt from Past Disasters? Analysis of the Mw 8.8 Mega Earthquake of Central Chile with MORT, Jordan Journal of Earth and Environmental Sciences (JJEES), 6, 1, 1-7, ISSN 1995-6681.

Araya, R. and Armen, D. K. (1988). Probabilistic Seismic Hazard Analysis with Improved Source Modeling Proceedings of Ninth World Conference on Earthquake Engineering, 8:81-86.

Arieh, E. and Rabinowitz, N. (1989). Probabilistic Assessment of Earthquake Hazard in Israel, Tectonophysics, 167: 223-233.

ASEZA (2010). A project on Support to building national capacity for earthquake risk reduction at ASEZA in Jordan, Disaster Risk Management Profile for Aqaba Special Economic Zone, Aqaba, Jordan.

Baaqeel, A. , Quliti, S. , Daghreri, Y. , Hajlaa, S. and Yami, H. (2016) Estimating the Frequency, Magnitude and Recurrence of Extreme Earthquakes in Gulf of Aqaba, Northern Red Sea. Open Journal of Earthquake Research, 5, 135-152. doi: 10.4236/ojer.2016.52011.

Boore, D.M. and Atkinson, G.M. (2008). Ground-Motion Prediction Equations for the Average Horizontal Component of PGA, PGV, and 5%-Damped PSA at Spectral Periods between 0.01 s and 10.0 s. Earthquake Spectra 24: (1) 99-138 https://doi.org/10.1193/1.2830434.

Campbell, K.W. and Bozorgnia, Y. (2014). NGA-West2 Ground Motion Model for the Average Horizontal Components of PGA, PGV, and 5% Damped Linear Acceleration Response Spectra. Earthquake Spectra, 30(3), pp.1087–1115. doi:10.1193/062913eqs175m.

Darvasi, Y., and Agnon, A. (2019). Calibrating a new attenuation curve for the Dead Sea region using surface wave dispersion surveys in sites damaged by the 1927 Jericho earthquake. Solid Earth, 10(2), 379-390.

Douglas, J., Bungum, H., and Scherbaum, F. (2006). Ground-motion prediction equations for southern Spain and southern Norway obtained using the composite model perspective. Journal of Earthquake Engineering, 10(01), 33-72.

El-Isa, Z.H., Merghelani, H.M. and Bazzari, M.A. (1984). The Gulf of Aqaba earthquake swarm of 1983 January-April. Geophysical Journal International, [online] 78(3), pp.711–722. doi:10.1111/j.1365-246x.1984.tb05066.x.

El-Isa, Z. H. and Al Shanti, A. (1989). Seismicity and tectonics of the Red Sea and western Arabia. Geophysical Journal International, 97 (3): 449-457, https://doi.org/10.1111/j.1365 246X.1989.tb00515.x.

Gardner, J.K. and Knopoff, L. (1974). Is the sequence of earthquakes in Southern California, with aftershocks removed, Poissonian? Bull Seismol Soc Am 64 (5): 1363–13667.

Garfunkel, Z., (1981). Internal structure of the Dead Sea Leaky Transform (rift) in relation to plate kinematics, Tectonophysics, 80: 81– 108.

Jaradat, R. Nusier, O. Awawdeh, M. Al-Qaryouti, M. and Fahjan, Y. (2008). De-aggregation of Probabilistic Ground Motions for Selected Jordanian Cities. Jordan Journal of Civil Engineering, (2): 173-196.

JBC- Jordanian Building Codes (2005) Ministry of Public Works and Housing, Amman-Jordan.

Konstantinos L., Domenico D. G., James H., and Dmitry A. S. (2019). The ISC Bulletin as a comprehensive source of earthquake source mechanisms. Earth Syst. Sci., 11, 565–578, https://doi.org/10.5194/essd-11-565-2019.

Klinger, Y., Rivera, L., Haessler, H. and Maurin, J.-C. (1999). Active faulting in the Gulf of Aqaba: New knowledge from the MW 7.3 earthquake of 22 November 1995. Bulletin of the Seismological Society of America, [online] 89(4), pp.1025–1036. doi:10.1785/bssa0890041025.

Mona Abdelazim, Mohamed N. El Gabry, Mohamed M. Gobashy, Mohamed H. Khalil, and Hesham M. Husseini, (2023). Seismicity and Fault Interaction in the Gulf of Aqaba. Pure Appl. Geophys, https://doi.org/10.1007/s00024-023-03279-x.

Mohammad Al-Adamat* and Abdullah Diabat (2022) "Results revealed the existence of a strike-slip regime in all stress tensors" Jordan Journal of Earth and Environmental Sciences (JJEES) (2022) 13 (4): 278-285 ISSN 1995-6681.

Najib Abou Karaki, Damien Closson and Mustapha Meghraoui, (2022) Seismological and Remote Sensing Studies in the Dead Sea Zone, Jordan 1987–2021, in M. M. Al Saud (ed.), Applications of Space Techniques on the Natural Hazards in the MENA Region, Springer Nature Switzerland AG 2022 https://doi.org/10.1007/978-3-030-88874-9_25.

Pascucci, M.W. F., and Lubkowski Z.A. (2008). Seismic Hazard and Seismic Design Requirements for the Arabian Peninsula Region. The 14thWorld Conference on Earthquake Engineering. Beijing-China. 24.

Paz M., and Leigh W., (2004). Structural Dynamics: Theory and Computation, 5th edition, ISBN 1- 4020-7667-3, Kluwer Academic Publishers.

Qadan, H. (1987). Probabilistic Study of Seismic Hazard in Jordan and Vicinity. Unpublished M.Sc. Thesis, Yarmouk University, Jordan.

Sbeinati M.R., Darawcheh R., and Mouty M., (2005). The historical earthquakes of Syria: an analysis of large and moderate earthquakes from 1365 B.C. to 1900 A.D. Science, Damascus University, Damascus, Syria, Annals of Geophysics, 48, 3.

Shaked, Y., Agnon, A., Lazar, B., Marco, S., Avner, U. and Stein, M. (2004). Large earthquakes kill coral reefs at the north-west Gulf of Aqaba. Terra Nova, 16 (3), pp.133–138. doi:10.111 1/j.1365-3121.2004.00541. X.

ten-Brink, U. and Ben-Avraham, Z. (1989). The anatomy of a pull-apart basin-seismic reflection observation of the Dead Sea basin, Tectonics, 8, 333-350.

USGS website (2020) Science of Changing World https:// earthquake.usgs.gov/earthquakes/search/ June 10, 2020 www. corssa.org/en/home/ last accessed 20th June 2021.

Yucmen, M.S, (1977). Source Modeling and Uncertainty Analysis in the Evaluation of Seismic Risk for Nuclear Power Plants, Research Report, Middle East Technical University, Ankara, Turkey.